FENOC
FirstEnergy Nuclear Operating Company

Beaver Valley Power Station
P.O. Box 4
Shippingport, PA 15077

Raymond A. Lieb
Director, Site Operations

724-682-7773
Fax: 724-643-8069

January 18, 2010
L-10-001

10 CFR 50.90

ATTN: Document Control Desk
U. S. Nuclear Regulatory Commission
Washington, DC 20555-0001

SUBJECT:
Beaver Valley Power Station, Unit No. 2
Docket No. 50-412, License No. NPF-73
Response to Request for Additional Information for License Amendment Request No. 08-027, Unit 2 Spent Fuel Pool Rerack (TAC No. ME1079)

By letter dated April 9, 2009 (Reference 1) as supplemented by letter dated June 15, 2009 (Reference 2), FirstEnergy Nuclear Operating Company (FENOC) requested an amendment to the operating license for Beaver Valley Power Station (BVPS) Unit No. 2. The proposed amendment would revise the Technical Specifications to support the installation of high density fuel storage racks in the BVPS Unit No. 2 spent fuel pool. By letter dated December 4, 2009 (Reference 3), the Nuclear Regulatory Commission (NRC) staff requested additional information to complete its review of the license amendment request.

The responses to the NRC request for additional information (RAI) are provided in the Attachment. The information provided by this submittal does not invalidate the no significant hazard evaluation submitted by Reference 1.

There are no regulatory commitments contained in this letter. If there are any questions or if additional information is required, please contact Mr. Thomas A. Lentz, Manager – FENOC Fleet Licensing, at 330-761-6071.

I declare under penalty of perjury that the foregoing is true and correct. Executed on January 18, 2010.

Sincerely,

Raymond A. Lieb

Raymond A. Lieb

A001
NRR

Attachment:
Response to December 4, 2009 NRC Request for Additional Information Related to Beaver Valley Power Station Unit No. 2 Spent Fuel Pool Rerack License Amendment Request

References:

1. FENOC Letter L-09-086, "License Amendment Request No. 08-027, Unit 2 Spent Fuel Pool Rerack," dated April 9, 2009 (Accession No. ML091210251).
2. FENOC Letter L-09-162, "Additional Technical Information Pertaining to License Amendment Request No. 08-027 (TAC No. ME1079)," dated June 15, 2009 (Accession No. ML091680614).
3. NRC Letter dated December 4, 2009, "BEAVER VALLEY POWER STATION, UNIT NO. 2 – REQUEST FOR ADDITIONAL INFORMATION RE: SPENT FUEL POOL RERACK LICENSE AMENDMENT (TAC NO. ME1079)," (Accession No. ML093280914).

cc: NRC Region I Administrator
NRC Senior Resident Inspector
NRR Project Manager
Director BRP/DEP
Site Representative (BRP/DEP)

To complete its review, the Nuclear Regulatory Commission (NRC) staff has requested additional information regarding FirstEnergy Nuclear Operating Company (FENOC) spent fuel pool rerack license amendment request (LAR) No. 08-027. The staff's request is provided below in bold text followed by the FENOC response for Beaver Valley Power Station (BVPS) Unit No. 2.

Mechanical and Civil Engineering Branch:

(Document reviewed: [Proprietary] Holtec Report No. HI-2084101, "Mechanical Drop Accident Analyses Supporting Beaver Valley Unit 2 Re-racking Project")

1. Section 1.2 (Scope)

a. State the basis for assuming a drop height of 24" above the top of the rack for the "shallow drop" event and the "gate drop" event.

Response:

It should be noted that Holtec Report HI-2084010 is the correct document number, not HI-2084101 as stated in the question. The fuel drop height (24") bounds the actual travel height of the fuel over the racks in the Beaver Valley Unit 2 Spent Fuel Pool (due to physical limitations such as hoist limit switches and the fuel handling tool height). As shown in Appendix C of Holtec Report HI-2084010, the fuel drop height (24") for the "shallow drop" event bounds the drop height (23.5") used in the drop analysis for the existing Beaver Valley Unit 2 spent fuel racks. Furthermore, the new racks are slightly taller than the existing racks, which would reduce the potential drop height.

Because the cask pit gate and transfer canal gate are considered "Heavy Loads", they are not permitted to travel over stored spent fuel at Beaver Valley Unit 2. Therefore, the "gate drop" event is a conservatively analyzed event that is not required because administrative actions (safe load paths) would prevent the event from occurring. A "gate drop" event was not performed nor required for the existing racks at Beaver Valley Unit 2 based on the above reason. The practice of FENOC personnel moving the gates is to minimize the lift height of the weir gate during installation and removal process in the fuel pool. The gate drop height (24") is consistent with the analysis from the Beaver Valley Unit 1 spent fuel pool rerack project.

b. State the basis for assuming a vertical drop of an empty rack from the top of the spent fuel pool water level.

Response:

The assumed rack drop orientation (vertical) is consistent with the rack lifting operation, and the assumed drop elevation (bottom of rack is four feet above the water level per HI-2084010), is conservative. It is possible that the rack could drop into the spent fuel pool water with a small inclination. However, as the rack moves downward in the water, the uneven pressures applied to the rack outer surfaces and interior cell wall surfaces due to the small inclination would force the rack to rotate to the vertical orientation where the rack experiences minimal drag force due to the smallest frontal area.

2. Section 4.3 (Material Properties)

a. Page 13 of 52 shows the true stress-true strain curve for SA240-304L. Provide the basis of this curve, or provide a copy of Reference 3.

Response:

Reference 3 is available on non-public NRC Agencywide Documents Access and Management System (ADAMS) with affidavit under accession number ML093570411.

b. Provide the true stress-true strain curve for SA564-630.

Response:

The true stress-strain curve for SA564-630 can be generated using the method described in the position paper (reference 3 in response to request for additional information [RAI] 2.a). Since the pedestal is not expected to experience significant stress, the more conservative bilinear material model based on the engineering stress/strain data was used in the analysis for simplicity. The bilinear material model requires input of Young's modulus, yield stress, failure strain and tangent modulus; the first three material data and the ultimate stress are listed in the first table in Section 4.3 of the report and are used to calculate the tangent modulus (tangent modulus=(140ksi-109.2ksi)/0.14in/in=2.2x10^5 psi/in/in).

c. Provide the bilinear engineering stress-strain relationship and its source for the weld material.

Response:

The weld material is conservatively assumed to be the same as the base metal (SA240-304L); the actual strength is much stronger than the base material. Therefore, the bilinear engineering stress-strain relationship (defined by Young's modulus, yield stress, failure strain and tangent modulus) for the weld material can be established using the four material properties shown in the first table in Section 4.3 of the report.

d. Provide the true failure strains and corresponding true stresses for the materials listed on page 12 of 52.

Response:

Two materials are listed on page 12 of the report. For material SA240-304L, the true failure strain and failure stress are calculated to be 1.204 and 126.4 ksi, respectively, as shown below. The true stress-strain curve is also shown in the figure in Section 4.3 of the report. For material SA564-630, engineering stress-strain relationship was used in the analysis as noted in Section 4.3 of the report and response to RAI 2.b.

SA240-304L

Per ASME code $s_y := 2.27 \cdot 10^4$ $s_u := 6.805 \cdot 10^4$ $E := 2.799 \cdot 10^7$

$n := 0.5$ Guess value

$$n := \mathrm{root}\left[s_u \cdot \left(\frac{e}{n} \cdot \ln\left(1 + \frac{s_y}{E}\right)\right)^n - s_y \cdot \left(1 + \frac{s_y}{E}\right), n\right] \qquad n = 0.235$$

$$K := \frac{s_u \cdot e^n}{n^n} \qquad q := 0.70 \qquad \varepsilon_y := \ln\left(1 + \frac{s_y}{E}\right) \qquad \varepsilon_f := \ln\left(\frac{1}{1 - q}\right)$$

$$K = 1.21 \times 10^5 \qquad q = 0.7 \qquad \varepsilon_y = 8.107 \times 10^{-4} \qquad \varepsilon_f = 1.204$$

$$\sigma_y := s_y \cdot \left(1 + \frac{s_y}{E}\right) \qquad \sigma_f := K \cdot \varepsilon_f^{\,n}$$

$$\sigma_y = 2.272 \times 10^4 \qquad \sigma_f = 1.264 \times 10^5$$

$i := 1 .. 7$

$$\varepsilon_i := \log(i + 3)^8 \cdot \left(\varepsilon_f - \varepsilon_y\right) + \varepsilon_y \qquad \sigma_i := K \cdot \left(\varepsilon_i\right)^n \qquad \varepsilon\_dyna_i := \varepsilon_i - \frac{\sigma_i}{E}$$

$$\varepsilon\_dyna = \begin{pmatrix} 0 \\ 0.02 \\ 0.067 \\ 0.16 \\ 0.311 \\ 0.529 \\ 0.824 \\ 1.199 \end{pmatrix} \qquad \sigma = \begin{pmatrix} 0 \\ 4.912 \times 10^4 \\ 6.462 \times 10^4 \\ 7.894 \times 10^4 \\ 9.213 \times 10^4 \\ 1.043 \times 10^5 \\ 1.157 \times 10^5 \\ 1.264 \times 10^5 \end{pmatrix}$$

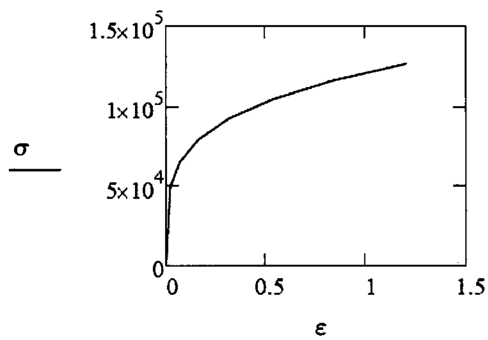

e. Page 13 of 52 lists the strain rate effect considered in the weld material model, which is based on actual test results for A36 steel. Provide the justification for applying these strain rate effects to stainless steel material, or provide the ADAMS Accession No. for the NRC safety evaluation report on Reference 4.

Response:

The ADAMS accession number for the NRC safety evaluation for safeguard report HI-2033134 could not be obtained. This report was prepared for the Private Fuel Storage (PFS) dry storage Atomic Safety and Licensing Board (ASLB) hearings. The use of A36 strain rate data for stainless steel is conservative since A36 is more brittle than stainless steel, which was accepted by the experts from the USNRC, Lawrence Livermore National Laboratory and Purdue University involved in the PFS dry storage ASLB hearings.

3. Section 7.1 (Analyses)

a. The acceptance criterion for the "shallow drop" accident is that the plastic deformation of the rack cell wall resulting from a fuel assembly drop event must not extend into the "poison zone." For this accident, the fuel assembly is assumed to hit a peripheral cell wall (filler panel). Figure 12, "Rack Plastic Strain," shows that the calculated fuel assembly displacement of 5.32 inches occurred by crushing the cell wall to a depth of 5.32 inches. The extent of plastic deformation measured from the rack top was determined as 17.91 inches. Provide the methodology and criteria used by LS-DYNA to determine these values.

Response:

Figure 11 shows the displacement time history of the dropped fuel assembly following the fuel-to-rack impact. The maximum displacement (5.32") reflects the total crush of the rack cell wall in the shallow drop event. Figure 12 plots the plastic strain distribution in the rack. The extent of plastic deformation is measured vertically from the top of the rack at a point away from the impact location to the depth where plastic strain reduces to zero. The measurement (17.91") is used to compare with the allowable (19.75") set forth in Section 2.2. LS-DYNA tracks the motion and calculates the stress/strain status of the model for the entire simulation duration. The LS-DYNA postprocessor can also measure the distance between any two nodal points based on the coordinates of the nodes. The LS-DYNA code has been independently validated under the Holtec Quality Assurance (QA) program and has been used for numerous NRC approved wet/dry storage projects.

b. Indicate if LS-DYNA was benchmarked for the case of edge crushing of a plate with boundary conditions as shown in Figure 12, or provide justification showing that these values are conservative, i.e., indicate if any tests or independent calculations were performed to provide assurance that the crushing depth and the extent of the plastic deformation as calculated by LS-DYNA have not been underestimated.

Response:

The LS-DYNA code has been independently validated and extensively used in many industries for predicting the impact damage in structures consisting of shells/plates. Due to the lack of data, however, Holtec has not been able to perform an LS-DYNA benchmark analysis specifically for the case of edge crushing of a rack cell wall. Nevertheless, the code has been benchmarked by Holtec against the test data obtained from the quarter–scale HI-STAR 100 impact limiter drop tests, which include various deformation and failure modes of thin shells. The Holtec benchmark analysis (HI-2073743) was reviewed and accepted by the USNRC, leading to the license approval of the HI-STAR 60 and HI-STAR 180 transport cask packages that are evaluated for drop events through LS-DYNA analysis in lieu of conducting drop tests. Moreover, the LS-DYNA code has been used in most of Holtec rack projects approved by the USNRC in the last decade.

c. The maximum effective plastic strain is shown as 0.513 in/in at element 2623. On page 12 of 52, the failure strain is listed as 0.4 in/in. Provide justification as to why the effective plastic strain is greater than the listed failure strain. Explain why the figure shows the largest strains in the range of 0.1027 - 0.1541 in/in.

Response:

The failure strain (0.4 in/in) listed on page 12 of the report is the engineering failure strain of the rack cell material (SA240-304L), which is much smaller than the corresponding true strain limit (described in response to RAI 2.d). The LS-DYNA material model for rack cells is based on the true stress-strain relationship of the material, and the LS-DYNA plastic strain results shown in Figure 12 represent the true plastic strain of the rack cells. The peak strain (i.e., 0.5137 in/in), which was only developed locally in element 2623, is not visible in the figure.

4. Appendix B: Impact Velocity Calculations

a. In equations A-3A on page B-2, state why the effect of the virtual mass is included in the equation for beta, when it is stated that the virtual mass is neglected for conservatism.

Response:

The variable ε in Equation A-3 represents both virtual mass and buoyant mass, which are considered to be identical numerically when the equation of motion (i.e., Equation A-1) is established. Equation A-3A on page B-2 was derived from equation A-3 by ignoring the contribution of the virtual mass (the denominator in the equation for beta is reduced from $1+\varepsilon$ to 1). Therefore, the variable ε remaining in Equation A-3A only reflects the contribution from the buoyant mass.

b. Provide a sketch of the transfer canal gate, and state why the thickness of 7.375 inches used in the calculation of the gate weight is conservative compared to 7.875 inches.

Response:

Based on the gate drawing shown in Ref. [5.1.12] of the report, a sketch of the gate with dimensions (including details showing that the gate is not solid steel) is provided below. The use of a smaller gate thickness reduces the frontal area of the dropped gate in water and hence conservatively reduces drag and increases impact velocity.

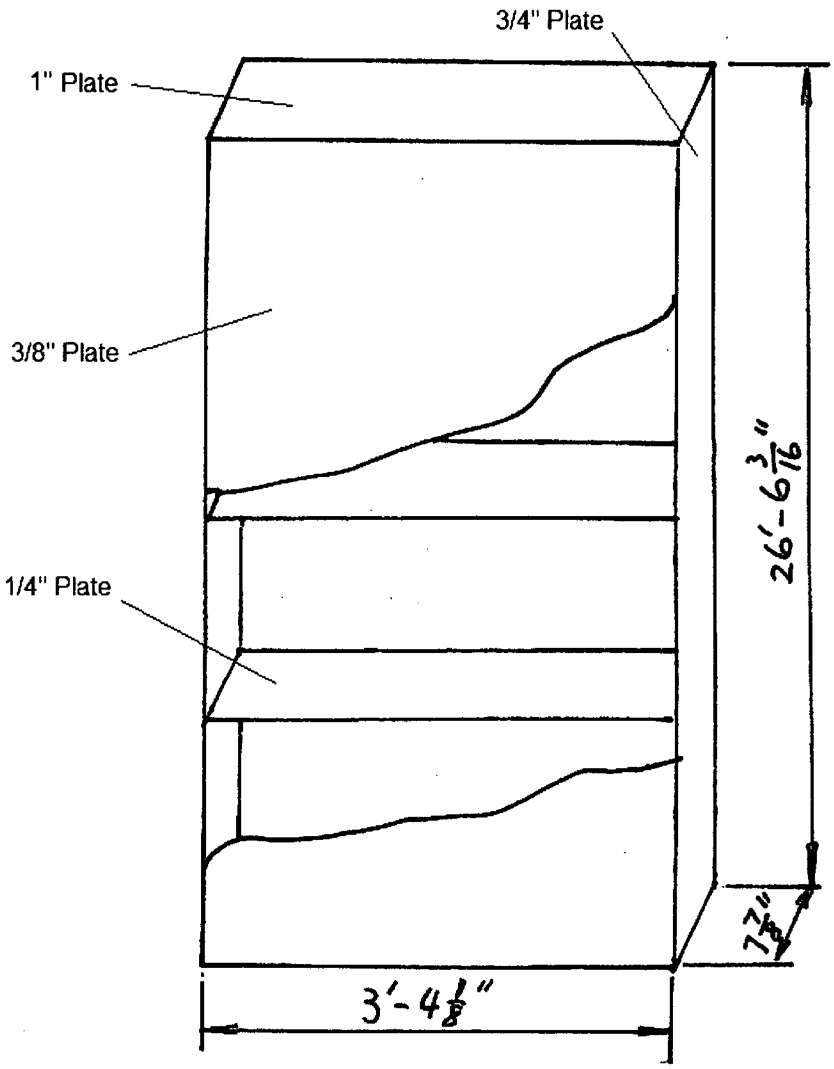

c. **Page B-18 shows the weight of the gate as 4020 pound-force (lbf). The length dimension is not given. Based on the dimension of the length provided on page 11 of 52, and using 7.375 inches for the thickness, the weight of the gate is calculated as 26,600 lbf. Provide a justification for the value given on page B-18, 4020 lbf.**

Response:

The cask pit gate and transfer canal gate are not constructed of solid steel. Source 1 of Reference [8] in Appendix B of the report documented an actual measured dry weight of 4020 lbf for the transfer canal gate, which is the larger gate.

The NRC staff has also reviewed Section 5.0, "Structural/Seismic Considerations" of Enclosure B of Reference 1 and [Proprietary] Holtec International Report No. HI-2084123, "Structural/Seismic Analysis for Beaver Valley Unit 2." The NRC staff

has identified the following additional information that is needed to complete its review of this report:

5. Provide the basis for the spring constants for the concrete slab and for the cellular structure on page A-6.

Response:

The spring constant for the concrete slab is calculated using the formula given in Reference [5-1] for the vertical stiffness of a rigid body of rectangular cross-section resting on a semi-infinite elastic foundation, which is expressed as:

$$k = \frac{E \cdot c_s \cdot A^{1/2}}{(1 - \nu^2)}$$

where E = elastic modulus of foundation
ν = Poisson's ratio of elastic foundation
A = cross-sectional area of rigid object with sides B and L
c_s = constant term which depends on aspect ratio of rigid object (B/L)

The following figure (which is reproduced from Reference [5-1]) shows the relationship between c_s and the aspect ratio (B/L).

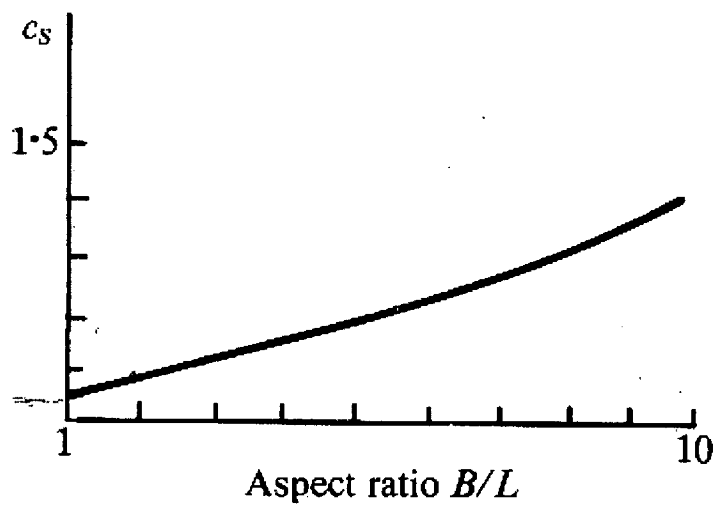

In Appendix A of Holtec Report No. HI-2084123, the concrete slab is considered as the elastic foundation, and the rack support pedestal is considered as the rigid object having an aspect ratio of 1.0 (c_s = 1.05). In Appendix A, the elastic modulus of concrete is taken as 1/15 times the elastic modulus of stainless steel. This lower bound estimate for the elastic modulus of concrete has a minor effect on the final pedestal spring rate since the final spring rate is dominated by the cellular structure.

The spring constant for the cellular structure is also calculated using the formula presented above with the following modifications. Since the cellular structure is not a solid body, the effective modulus of the cellular structure is taken as the Young's modulus of stainless steel multiplied by the ratio of the metal area of a single cell versus the enclosed area of a single cell. A reduction factor of 0.25 is also applied to the final result to account for the fact that the pedestals are located at the rack corners, which means that the cellular structure has the characteristics of a "quarter space".

References:

[5-1] Levy, S. and Wilkinson, J., The Component Element Method in Dynamics, McGraw-Hill, Inc., 1976.

6. Reference 5 stated that "In specific design applications, the authors have used four beam elements and five nodal points to represent the rack structure." Provide justification for representing the model of a generic rack module by a single beam and two nodes in the Beaver Valley Unit 2 seismic analysis.

Response:

The use of a single beam and two nodes to model a Beaver Valley Unit 2 rack module is justified because the lowest natural frequency of the rack cellular structure is above 33 Hz. The lowest natural frequency is conservatively calculated assuming that the rack cellular structure acts like a cantilever beam. In reality, the spent fuel racks are freestanding; thus, the rack cellular structure acts more like a free-free beam, which would increase the lowest natural frequency as compared to the calculated value below.

$L := 168.625\text{in}$	Total length of rack cells above base plate (per Ref. [6-1])
$W := 21400\text{lbf}$	Bounding weight of Beaver Valley Unit 2 rack module (per Ref. [6-1])
$w := \dfrac{W}{L}$	Weight per unit length of rack cellular structure
$I := 53319\text{in}^4$	Area moment of inertia of rack cell cross-section (minimum value for all racks)
$E := 27.6\,10^6 \cdot \text{psi}$	Young's modulus of SA-240-304L at 200F (per Ref. [6-2])

Per Table 36 (case no. 3b) of Reference [6-3], the lowest natural frequency of a uniform cantilever beam is:

$$K_1 := 3.52$$

$$f_1 := \frac{K_1}{2\cdot\pi}\cdot\sqrt{\frac{E\cdot I\cdot g}{w\cdot L^4}} \qquad f_1 = 41.7\text{Hz}$$

Since the calculated frequency of the rack module is above 33 Hz, and the energy associated with the earthquake lies below 10 Hz, the use of a single beam and two nodes is sufficient to predict the rack deformation due to the design basis Safe Shutdown Earthquake (SSE).

References:

[6-1] Holtec Drawing No. 5606, “Spent Fuel Pool Layout”, Rev. 5.

[6-2] ASME Boiler & Pressure Vessel Code, Section II, Part D, 1998 Edition.

[6-3] Young, W., Roark’s Formulas for Stress & Strain, McGraw-Hill, Inc., 6th Edition.

7. Provide the method for calculating the mass matrix for the single beam and two nodes.

Response:

In the Whole Pool Multi-Rack (WPMR) model, the cellular structure of each rack module is represented by two lumped masses joined by a single beam element, as depicted below.

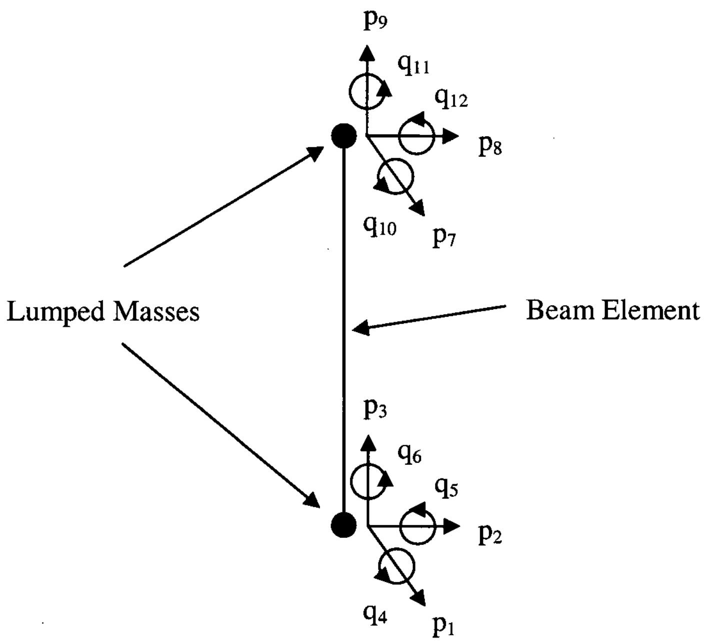

The lumped masses each have six degrees of freedom (DOF): they can translate in three orthogonal directions (e.g., p_1, p_2, p_3 in the above diagram) and rotate about three axes (e.g., q_4, q_5, q_6 in the above diagram). The beam element, which is comprised of six linear springs simulating shear and bending in two planes, extension, and torsion, is massless. The mass matrix for the single beam and two nodes is defined as follows (neglecting fluid mass terms):

$$[M]=\begin{bmatrix} m_1 & 0 & 0 & 0 & 0 & 0 & 0 & 0 & 0 & 0 & 0 & 0 \\ 0 & m_2 & 0 & 0 & 0 & 0 & 0 & 0 & 0 & 0 & 0 & 0 \\ 0 & 0 & m_3 & 0 & 0 & 0 & 0 & 0 & 0 & 0 & 0 & 0 \\ 0 & 0 & 0 & I_4 & 0 & 0 & 0 & 0 & 0 & 0 & 0 & 0 \\ 0 & 0 & 0 & 0 & I_5 & 0 & 0 & 0 & 0 & 0 & 0 & 0 \\ 0 & 0 & 0 & 0 & 0 & I_6 & 0 & 0 & 0 & 0 & 0 & 0 \\ 0 & 0 & 0 & 0 & 0 & 0 & m_7 & 0 & 0 & 0 & 0 & 0 \\ 0 & 0 & 0 & 0 & 0 & 0 & 0 & m_8 & 0 & 0 & 0 & 0 \\ 0 & 0 & 0 & 0 & 0 & 0 & 0 & 0 & m_9 & 0 & 0 & 0 \\ 0 & 0 & 0 & 0 & 0 & 0 & 0 & 0 & 0 & I_{10} & 0 & 0 \\ 0 & 0 & 0 & 0 & 0 & 0 & 0 & 0 & 0 & 0 & I_{11} & 0 \\ 0 & 0 & 0 & 0 & 0 & 0 & 0 & 0 & 0 & 0 & 0 & I_{12} \end{bmatrix}$$

where:

$$m_1 = m_2 = m_3 = m_7 = m_8 = m_9 = \frac{W}{2 \cdot g}$$

$$I_4 = I_{10} = 0.5\left[\frac{1}{12}\left(\frac{W}{g}\right)\left(b^2 + h^2\right)\right]$$

$$I_5 = I_{11} = 0.5\left[\frac{1}{12}\left(\frac{W}{g}\right)\left(a^2 + h^2\right)\right]$$

$$I_6 = I_{12} = 0.5\left[\frac{1}{12}\left(\frac{W}{g}\right)\left(a^2 + b^2\right)\right]$$

W = empty weight of rack module

a = rack module size in the x-direction

b = rack module size in the y-direction

h = rack cell height

8. Provide a description of the method for determining the impact of the fuel masses and the single beam rack module.

Response:

Impacts between the lumped fuel masses and the single beam representing the rack cellular structure are determined through the use of non-linear compression-only spring elements (referred to as fuel-to-cell impact springs). There are four such compression-only springs surrounding each of five fuel masses (as described in Figure 5.2 in Enclosures B and C of FENOC letter L-09-086 dated April 9, 2009). At the start of the simulation (t = 0 sec), the lumped fuel masses are centered between the fuel-to-cell impact springs such that the clearance gap is the same in all four directions. As the simulation proceeds, the displacement at each degree of freedom in the Whole Pool Multi-Rack (WPMR) model is calculated using a central difference algorithm. For each time step, the clearance gaps between the lumped fuel masses and the rack cell walls are updated based on the current Degree of Freedom (DOF) solution. If a clearance gap drops below zero at any of the 20 fuel-to-cell wall impact spring locations, then a fuel-to-cell wall impact occurs at that time instant. In other words, a negative gap value indicates that the fuel-to-cell wall impact spring is compressed. The instantaneous impact force is equal to the compression of the fuel-to-cell wall impact spring times the spring rate.

The gap value at each fuel-to-cell wall impact spring location is a time varying function of the horizontal displacement of the fuel mass and the lateral displacement/deflection of the single beam rack module at the corresponding fuel mass elevation. The lateral displacement/deflection of the single beam rack module at any elevation is determined from the end node displacements (RAI Question 7 response contains DOFs ascribed to end nodes) in conjunction with the shape function for the beam element, which is derived from Reference [8-1].

References:

[8-1] Levy, S. and Wilkinson, J., The Component Element Method in Dynamics, McGraw-Hill, Inc., 1976.

(Document Reviewed: [Proprietary] Holtec Report No. HI-2084123)

9. Figures

Figure 1.1 shows that the corners of some racks don't match, so that impact could occur somewhere between the corners of one of the racks. An example is a corner of Rack A-3 impacting the middle of the top of Rack B-3, and a corner of Rack B-3 impacting Rack A-3 one cell length from the corner. Since impact between racks is assumed to occur at the corners only, provide the method for determining the impact loads for impact that does not occur at the corners.

Response:

In order to simulate the potential for rack-to-rack and rack-to-wall contact, compression-only gap elements are positioned at the corners of every rack in the Whole Pool Multi-Rack (WPMR) model, regardless of the rack alignment. Thus, the model is capable of determining impact loads that occur between a rack corner and the side wall of an adjacent rack (i.e., between the corners). To clarify further, the following sketch shows the locations of the compression-only gap elements between Racks A2, A3, B2, and B3, which are included in the Beaver Valley Unit 2 WPMR model. The compression only gap elements that track potential impacts between a rack corner and an adjacent rack side wall are labeled as A through F.

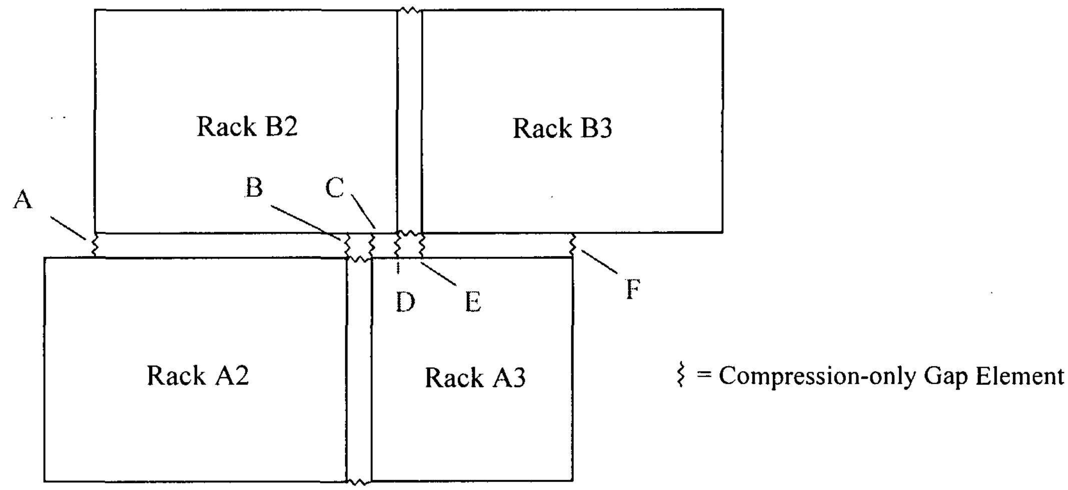

A compression-only gap element transmits a force only when the gap between racks at that particular location reduces to zero as a result of the seismic motion. Based on the WPMR simulations performed in Holtec Report No. HI-2084123 (Structural/Seismic Analysis for Beaver Valley Unit 2), rack-to-rack impacts do occur at locations A, B, E, and F; the maximum impact force is 43,570 lbf, which occurs at location B. There are no rack-to-rack impacts at locations C and D in any of the WPMR simulations.

10. Appendix A

Page A-8

a. **In the calculation of the compression spring stiffness for rack-to-rack top impacts, provide the basis for assuming a characteristic length of 3-cell inside diameters and 1-cell depth for the vertical distance.**

Response:

A characteristic depth of one cell inside dimension (ID) (8.8") is assumed in the calculation of the compression spring stiffness for rack-to-rack impacts because it is roughly equal to the vertical length of the tie-bars (8.0") that form the connections between adjacent cells. In the horizontal direction, the rack-to-rack impact load will spread across the entire width of the rack. However, the characteristic length used in the calculation of the compression spring stiffness should not exceed 50% of the rack width since there are two compression-only gap elements along each line of impact (i.e., one at each corner). For conservatism, the compression spring stiffness is calculated in Appendix A based on a characteristic length of three cell IDs, which is less than the half-width of the smallest spent fuel rack in the pool (Rack A3 has a half-width of four cell IDs). The use of a shorter length and a larger depth is conservative because it overestimates the spring stiffness, which typically results in higher impact loads. This modeling approach is consistent with other spent fuel rack licensing applications (as detailed in Table 5.4.1 in Enclosure B of FENOC letter L-09-086 dated April 9, 2009).

b. Provide the basis for the formula for the damping values.

Response:

The damping formula on page A-8 is related to the Holtec proprietary computer code SPG16, which is a pre-processor code used to generate the compression-only gap elements for the WPMR model. The computer code SPG16 computes the damping coefficient for the compression-only gap elements as a function of the damping coefficient for the rack beam element. As a result, the input file for the computer code SPG16 requires the damping value for compression-only gap elements be specified in the form:

$$dpc = 1 - \frac{0.10}{\xi}$$

where ξ is the damping ratio for the rack beam elements (β is substituted for ξ on page A-8). The 0.10 value appears in the above formula to account for the non-linear impact occurring at rack-to-rack/wall interfaces during an earthquake. In other words, the damping percentage at these interfaces is artificially set at 10%. This value is not to be interpreted as a measure of internal damping, rather as a "pseudo damping" value that enables a conservative solution of a non-linear dynamics problem using a simplified model. This approach has been used previously by Holtec for numerous spent fuel rack licensing applications (as detailed in Table 5.4.1 in Enclosure B of FENOC letter L-09-086 dated April 9, 2009).

<u>**Page A-11**</u>

c. Provide the basis for the formula for the structural damping multiplier.

Response:

The formula for the structural damping multiplier is based on the principle of Rayleigh Damping, where the damping matrix of the system is given as:

$$[C] = \alpha[M] + \beta[K] \qquad (1)$$

and [M] = mass matrix of the system; [K] = stiffness matrix of the system; α and β are constants.

In the Whole Pool Multi-Rack (WPMR) analysis performed for Beaver Valley Unit 2, as well as previous WPMR analyses for other sites (as detailed in Table 5.4.1 in Enclosure B of FENOC letter L-09-086 dated April 9, 2009), the value of α is conservatively set to zero. Therefore, the formula for the damping matrix simplifies to:

$$[C] = \beta[K] \qquad (2)$$

For a one degree of freedom spring-mass-damper system, the scalar damping coefficient, c, can be expressed as:

$$c = 2 \cdot \xi \cdot \sqrt{m \cdot k} = 2 \cdot \xi \cdot \sqrt{\frac{m}{k}} \cdot k \qquad (3)$$

where m is the mass, k is the spring constant, and ξ is the damping ratio. Substituting $2 \cdot \pi \cdot f = \sqrt{\frac{k}{m}}$ and rearranging Equation (3) yields:

$$c = \frac{\xi}{\pi \cdot f} \cdot k \qquad (4)$$

where f is the frequency for damping.

From Equations (2) and (4), the formula for β for a spring-mass-damper system is:

$$\beta = \frac{\xi}{\pi \cdot f} \qquad (5)$$

This is the formula used in Appendix A of Holtec report HI-2084123 to calculate the structural damping multiplier.

11. Appendix D

<u>**Page D-18**</u>

a. **The highest impact load is determined as occurring between Racks A-2 and A-3. Provide the basis for assuming that 8 compression members (cell walls) are available to resist the rack-to-rack impact load of 108,430 lbf, when impact is assumed to occur at the cell corners only.**

Response:

The maximum rack-to-rack impact load of 108,430 lbf is the bounding impact load at the northeast and southeast corners of Rack A2 with the northwest and southwest corners of Rack A3, respectively. Since the impact occurs simultaneously at both corners, the impact load is distributed over the entire face of the rack (i.e., the east face of Rack A2 and the west face of Rack A3). Thus, all of the cell walls that are normal to the impact face act in compression to resist the impact load. Although the calculation in Appendix D only credits 8 cell walls, there are actually 10 cell walls on Rack A2 (and Rack A3) that are perpendicular to the impact face plus 2 reinforcement bars (or bumper bars).

The value in Appendix D (108,430 lb) is conservative since it equals the sum of the maximum impact forces for each spring regardless of time. In other words, the two spring forces that are summed together to yield 108,430 lb do not occur at the same time instant. When the two spring forces are added as a function of time, the maximum instantaneous impact load between Rack A2 and Rack A3 is 101,800 lbf.

During the review of the analysis to support the response to this RAI on Appendix D, a determination was made that the supporting analysis was non-conservative. Based on this determination, the supporting analysis had to be re-performed and resulted in a modification to the rack reinforcement bars at the rack top around the entire perimeter. In the latest revision to HI-2084123 (Rev. 3), the rack-to-rack impact evaluation in Appendix D has been deleted and replaced by a new evaluation in Appendix H, which utilizes the finite element code LS-DYNA (as described in response to RAI 11.c). Note that the finite element model analyzed in Appendix H uses the available 10 cell walls and 2 reinforcing (bumper) bars in the new analysis.

b. Provide a sketch showing the configuration chosen for determining the compression stresses. Indicate the location of the "reinforcement bar thickness," which is not included in the description of the rack modules.

Response:

The following sketch shows the impact load being applied to Rack A2. The reinforcement bars, which are made from ¼" thick stainless steel plate (SA240-304), are welded to the exterior cell walls around the entire rack perimeter. The reinforcement bars are located ¼" below the top of the rack, and they have a depth of 10 inches.

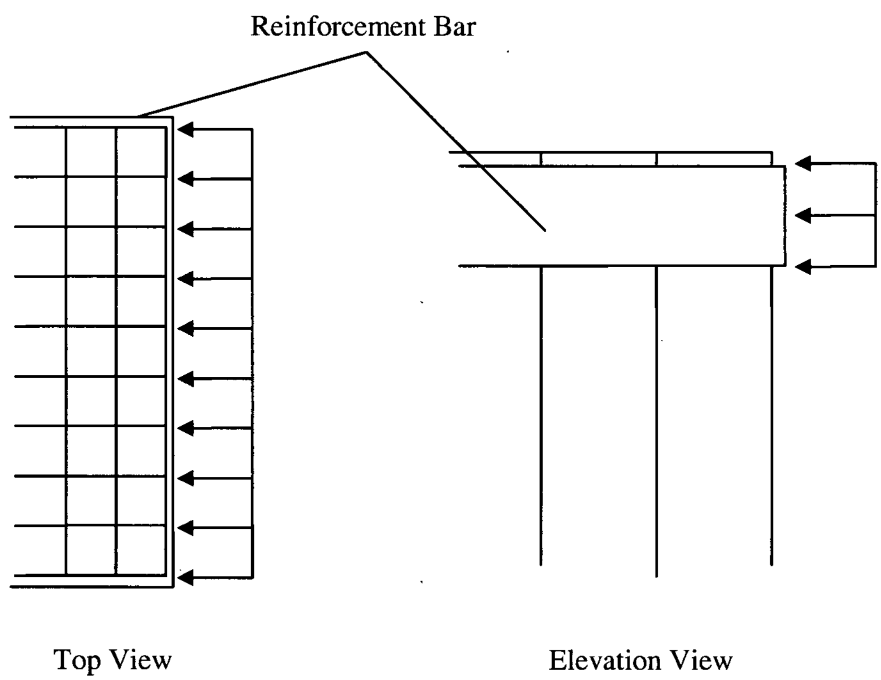

Page D-19

c. **Provide the basis for assuming "all edges clamped" plates in the buckling analysis, when at least one of the cell edges is free.**

Response:

As noted in the response to RAI 11.a, the buckling analysis has been re-performed and replaces the analysis referenced in the original submittal. The new analysis is performed using the Holtec QA validated commercial finite element code LS-DYNA, which is the same code used in the mechanical drop accident analysis for the Beaver Valley Unit 2 spent fuel racks. The objective of the analysis is to demonstrate that the rack cell structure will not buckle under 1.5 times the maximum impact load, as required by Section III, Appendix F, F-1331.5 of the American Society of Mechanical Engineers (ASME) code. Figure 11-1 shows the LS-DYNA model for evaluating the rack that experiences the maximum impact force in the spent fuel pool. The rack model for the rack-to-rack impact analysis is obtained by modifying the existing rack model developed for the Beaver Valley Unit 2 mechanical drop accident analysis. The model modification reflects the latest rack design improvement, namely adding 0.25"(thick)x10"(wide) reinforcement bars at the rack top around the entire perimeter. The LS-DYNA model takes advantage of the symmetry of the impact problem by applying appropriate boundary conditions and adjusting the cell wall thickness at the symmetry plane. As shown in the model, the top of the impacted rack is in contact with a 10" wide rigid rectangular plate, which represents the impactor (i.e., the adjacent rack reinforcement bar) in a rack-to-rack impact event. The bounding impact force time history is obtained from the Whole Pool Multi-Rack (WPMR) analysis and has a calculated value of 101.8 kips. To develop a load sufficient to cause deformation of the impactor, the impact time history is further amplified by a factor of 2 (such that it has a peak value of 203.6 kips), and that load is applied to the back surface of the rigid impactor as a uniform pressure. Figure 11-2 shows the amplified impact force time history applied to the rack top. Analysis using this time history impact loading provides a displacement time history of the impactor for the analyzed rack-to-rack top impact, presented in Figure 11-3, which shows no deformation occurring until time equals 0.0325 seconds when the impact force reaches 153.5 kips. At the time that the maximum impact load (101.8 kips) is reached, there is no permanent deformation in the rack cells as shown in Figure 11-4. Based on the amplified input impact force time history shown in Figure 11-2, the safety factor against buckling is determined as follows.

Impact Force at Buckling	Maximum Impact Force	Safety Factor
153.5 kips	101.8 kips	1.51

The calculated safety factor against impact buckling is obtained by dividing the impact force at buckling with the peak impact force experienced by the rack during the SSE event. The calculated safety factor of 1.51 exceeds the minimum required value per Appendix F, F-1331.5 of the ASME Section III Code. Therefore, the rack design can safely withstand the maximum rack-to-rack impact load.

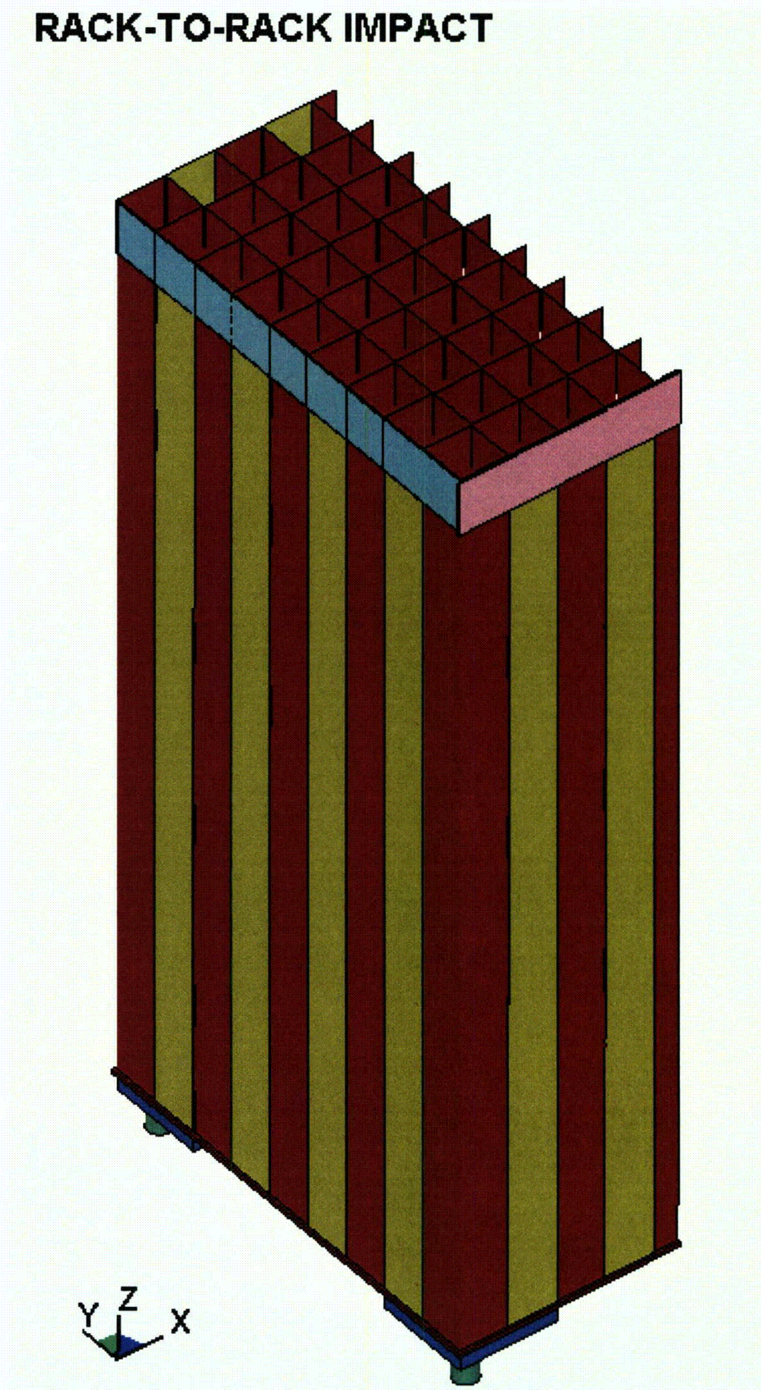

Figure 11-1: Rack-to-Rack Impact LS-DYNA Model – Beaver Valley Unit 2 Rack

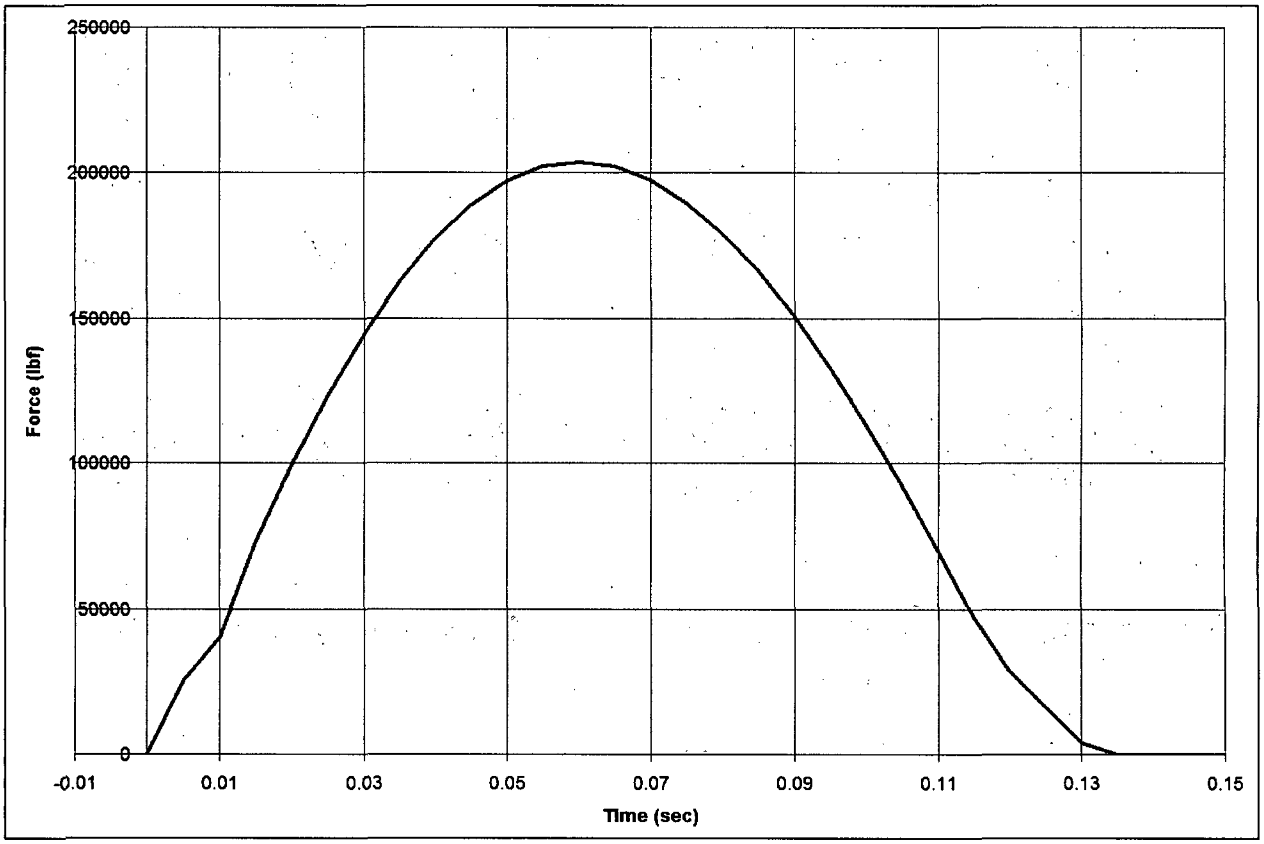

Figure 11-2: Input Force Time History for Rack-to-Rack Impact Analysis

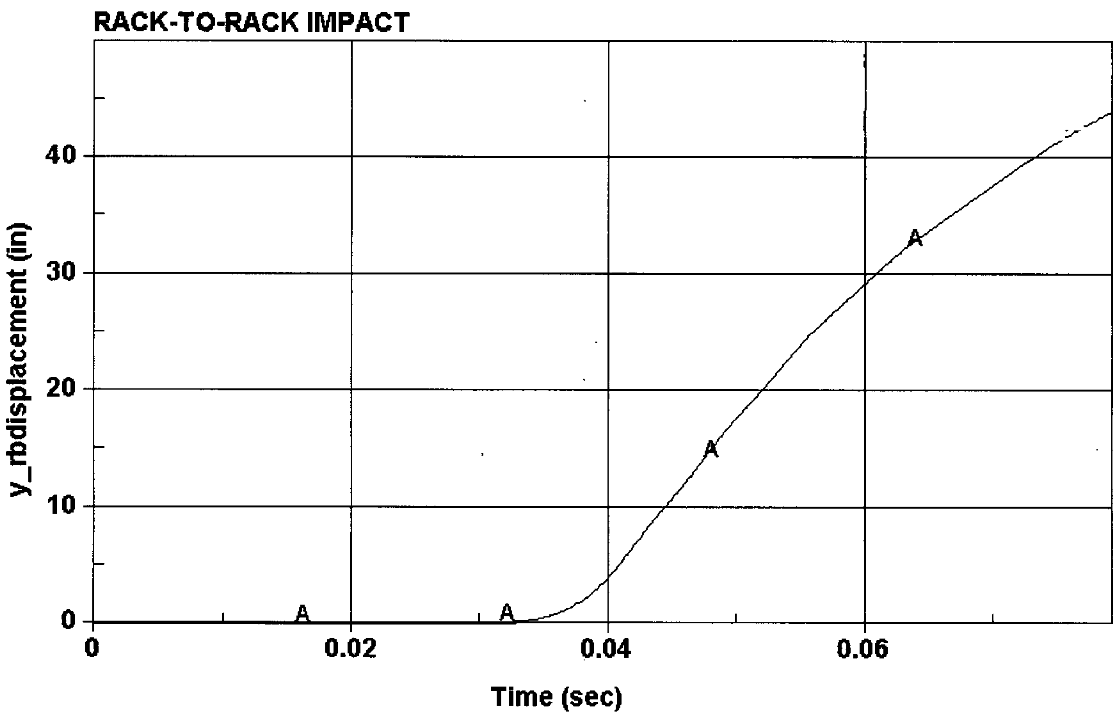

Figure 11-3: Displacement Time History of the Impactor – Rack Top Impact

Figure 11-4: Plastic Strain Distribution in Rack Under the Maximum Impact Load

<u>Balance-of-Plant Branch</u>

12. In Section 6 of Enclosure B to Reference 1, the criteria for bulk pool temperature is defined to be 170°F for case 1 and 173°F for case 2. In both cases, the local temperature in the rack cells shall be demonstrated to be below the local saturation temperature. These criteria are applicable to all rack areas in the pool.

As part of the installation of new racks in the BVPS-2 SFP, a new rack will be temporarily placed in the cask pit area. On page 6-13 of Enclosure B to Reference 1, it is stated that, "An additional CFD model of the rack in the cask pit was constructed and analyzed, and demonstrated that the rack in the cask pit condition is bounded by the normal condition with all racks in the SFP." However, no additional detail is provided.

Provide further description of the analysis performed and results obtained from the modeled fuel rack in the cask pit area demonstrating that there is adequate cooling flow to the cask pit area, that pool temperatures within the cask pit will remain within allowable values, and that local temperature in the rack shall be below the local saturation temperature.

Response:

Section 6 of Enclosure B described the methodology and major assumptions applied to the analysis of temperatures in the Spent Fuel Pool (SFP). These same methodologies and assumptions were used to evaluate the temperatures in the new rack when it is temporarily placed in the cask pit and loaded with spent fuel. A description of this analysis is provided below.

The SFP bulk temperature analysis described in Section 6 of Enclosure B is directly applicable to the cask pit. This evaluation assumed all of the decay heat that could possibly exist in the new racks (all storage locations filled), regardless of whether the one rack is in the SFP or in the cask pit, and conservatively neglects any thermal capacity contribution of the cask pit water.

Because the cask pit is adjacent to the SFP, connected only by the gate opening, a specific local temperature evaluation of the rack in the cask pit was necessary. To perform the needed analysis, a three-dimensional model of the cask pit containing the new rack was constructed using the same FLUENT code used to perform the local temperature of the new rack array in the SFP. The model includes both the cask pit itself, with recognition of the difference in floor elevation in the shallow and deep ends of the pit, and the gate opening that connects the cask pit to the SFP. The rack is modeled as a porous medium with a specified volumetric decay heat load, the same methodology used in modeling the racks in the SFP.

The loads and boundary conditions are as follows. First, the volumetric decay heat in the rack in the cask pit assumes that the fuel assemblies are cooled for either 18 months (one refueling batch) or 36 months (balance of fuel in the rack). During the installation, the fuel placed in the cask pit will be confirmed to have at least these cooling times. The cask pit walls and floor are assumed insulated; the same condition applied in the model of the racks in the SFP. The end of the gate opening that connects the cask pit to the SFP is set as a boundary with a temperature fixed to 170°F, the maximum computed SFP bulk temperature. Water is free to flow across this boundary as driven by buoyancy, with water entering at 170°F.

The solution of this model determined that the maximum local water temperature in the cask pit would be less than 177°F, which is lower than the corresponding value for the racks in the SFP and considerably lower than the allowable limit of 240°F (local saturation temperature) stated in Section 6 of Enclosure B. Therefore, the cooling flow to the cask pit area is adequate.

The difference between the local water temperature in the cask pit rack and the adjacent fuel cladding (i.e., the clad superheat) was calculated using the same methodology used to calculate this value for the racks in the SFP, although the fuel decay heat was reduced to correspond to 18-month cooled fuel. Adding the result to the maximum local water temperature in the cask pit yielded a maximum fuel cladding temperature less than 179°F, which is lower than the corresponding value for the racks in the SFP and considerably lower than the allowable limit of 240°F stated in Section 6 of Enclosure B.

These considerations are the basis for the statement in Section 6 of Enclosure B.

References

1. **Letter of April 9, 2009, from Peter. P. Sena, III, FENOC, to Document Control Desk, with Enclosure B, "Holtec Licensing Report for Beaver Valley Unit 2 Rerack (Proprietary Version)."**

2. **Holtec Report HI-2084010, "Mechanical Drop Accident Analyses Supporting Beaver Valley Unit 2 Reracking Project," March 3, 2009.**

3. **HI Position Paper DS-307, "Construction of True Stress-True Strain Curve for LS-DYNA Simulations," Rev. 2.**

4. **Holtec Report HI-2033134 (Safeguards), "Updated Structural Evaluation of an F-16 Aircraft Impact on HI-STORM Overpacks at the PFS Facility," Rev. 2.**

5. **Soler, A. I., and Singh, K. P., "Seismic Response of a Free Standing Fuel Rack Construction to 3-D Floor Motion," Nuclear Engineering and Design, 80 (1984).**